

A STOCHASTIC STRUCTURE MODEL FOR PREDICTING SHEET CONSOLIDATION AND PRINT UNIFORMITY

François Drolet¹ and Tetsu Uesaka²

¹Pulp and Paper Research Institute of Canada, Pointe-Claire, Qc, Canada

²Mid Sweden University, FSCN, Sundsvall, Sweden

ABSTRACT

The microscopic response of a paper sheet to compressive forces is of great importance in predicting print quality as well as the sheet structures developed in wet pressing and calendering. In this report, we propose a new compression model that preserves the entire three-dimensional, stochastic, fibre network structure. The model includes Z-directional deformation of fibres in both compressive and shear modes. Permanent deformation of each fibre (such as caused by fibre collapse) can be achieved by adjusting the stiffness of the fibre during compression or unloading. The stiffness of the plates can also be chosen to represent, for example, a hard printing plate, a blanket, or a soft-nip calendar cover. Although we still need to collect basic fibre stiffness data in order to perform quantitative comparisons between model predictions and experimental results, simulated structures already show typical features of consolidated paper sheets. As a first application, we study the contact mechanics between a printing plate and a model paper structure

INTRODUCTION

One of the outstanding issues in printing research is to predict print defects and print non-uniformity, such as mottles and missing dots, in terms of surface and bulk properties of paper. It has been increasingly recognised that surface roughness and formation are *not* sufficient parameters for describing various print non-uniformity issues. The best way to investigate this problem may be to directly observe the uniformity of contact between the paper surface and the rigid/soft printing plates, as well as the corresponding paper deformation within the printing nip. Because of the experimental difficulties and the stochastic nature of paper structures, attempts to do this have met with limited success [1, 2]. An alternative is to construct a model that captures the most important aspects of paper structure and nip impressions. Ideally, such a model would also include a description of ink transfer, and account for the influence of ink properties on print uniformity.

The Pakka model [3] is one of the best known numerical models for simulating the three-dimensional structure of paper. In this approach, fibre networks are formed by depositing fibres one by one randomly over a flat substrate. The structural properties of the final network depend on the dimensions of the fibres as well as on their flexibility. Recently, Provatas and Uesaka [4] extended the approach to include the effect of consolidation on sheet structure. This is an important addition to the model since all paper-making processes involve one or more consolidation steps such as couching, wet pressing, and calendering. Furthermore, sheet deformation under compression has direct relevance to the paper-plate contacts in a printing nip.

In the model of Provatas and Uesaka [4], a deposited fibre network was replaced with a set of springs placed on a rigid foundation. Non-uniform consolidation was represented by the deformation of the (coarse-grained) spring elements whose mechanical properties were determined by the local density. The main drawback to this approach is that it neglects fibre-level deformations inside the sheet structure. In this paper, we propose a new consolidation model that retains the entire three-dimensional structure of the deposited fibre network and provides a more realistic description of how it deforms under compression.

BACKGROUND

The physical properties of a sheet of paper depend on the properties of the fibres of which it is made as well as the geometrical arrangement of these fibres in the sheet. In many applications, the performance of the paper is

determined primarily by its structural properties. As a result, it is of great importance to understand which structural characteristics are most relevant for a given application and to predict, if possible, how these characteristics change with the properties of the fibres or the details of the papermaking process. Kallmes and Corte [5, 6] were among the first to describe the statistical geometry of two-dimensional random fibre networks. Starting from a few, simple assumptions about the way the fibres deposit to form a network, they derived expressions predicting how properties such as the total number of fibre crossings or the mean free fibre length change with the number of fibres in the network and their dimensions. They found good agreement between their predictions and experimental values obtained from handsheets of very low basis weight. Most attempts to generalize their approach to three dimensions have treated paper as a laminate of “two-dimensional” layers, with some interaction parameters between the layers (see, for example, [7]). With this approach, it was possible to calculate analytically quantities such as the variance of local density [8] and the fractional contact area of fibres [9].

A more direct approach to predicting the statistical properties of three-dimensional paper structures is to integrate the most important aspects of the papermaking process into a simulation tool that can be used to generate three-dimensional fibre networks [3, 10]. The Pakka model of Alava and Niskanen [3] is one example of this approach, in which fibres are deposited one by one and independently of each other, as if sedimenting from a very dilute pulp suspension. The fibres are modelled as straight beams oriented along either the X or Y axis. Bending forces caused by water drainage are taken into account by assigning a flexibility parameter T_f to the fibres which are allowed to bend downwards around fibre-fibre bonds. In the limit of long fibres, it can be shown that the network properties depend only on the dimensionless parameter $F = T_f w_f / t_f$, where w_f and t_f are the width and thickness of the fibres, respectively. Niskanen et al. [11] found that the relative bonded area of simulated sheets increases linearly with F while the distribution of pore heights is roughly exponential. Several improvements and generalizations of the Pakka model have been proposed over the years. For instance, it is straightforward to mix fibres from different species and to include all possible orientations in the XY plane. It is also possible to align the fibres preferentially along one direction and to mimic the effects of hydrodynamic smoothing or fibre flocculation [12].

Perhaps the greatest limitation of the Pakka model is that it does not directly include the effect of consolidation, even though it is an essential part of both the papermaking and printing processes. In the model, the effects of consolidation were introduced by flexing the deposited fibres in the thickness direction of the sheet, i.e., by making fibres more flexible. As a result, the

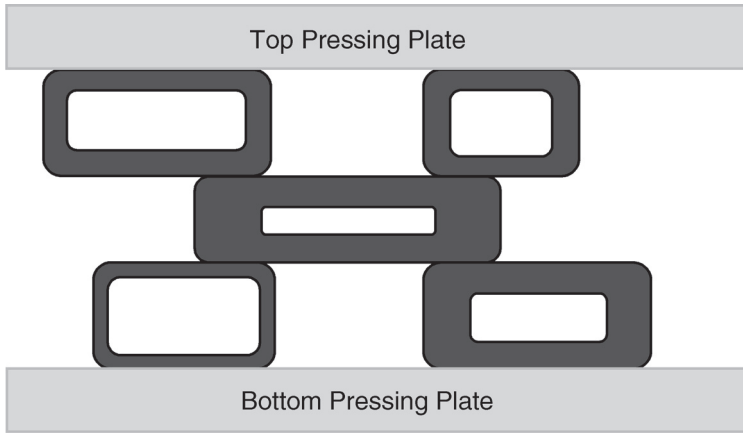


Figure 1 Cross-sectional view of a small fibre network in contact with two pressing plates.

structures created by this algorithm can be highly tortuous depending on the final density to be achieved. The model yielded almost equal to or even higher permeability in the thickness direction than in the plane of the paper. This is contrary to experimental results, as indicated by Aaltosalmi and coworkers [13]. To address this limitation of the PAKKA model, Provatas and Uesaka recently proposed a model that takes deposited fibre networks as input and compresses them to a given thickness or pressure. To illustrate how the model works, we have drawn in Figure 1 a cross-sectional view of a small fibre network in contact with two flat pressing plates and shown in Figure 2 how that system would be discretized using their approach. During compression, the bulk structure of the network is replaced by a set of independent, vertical springs connecting the top surface of the paper to the bottom plate, which is rigid and remains fixed during compression. The stiffness of individual springs inside the paper is determined from the local mass density, averaged over the thickness of the structure. In Figure 2, we have used thicker lines to draw springs with a high stiffness. As shown in the figure, the top pressing plate is also decomposed into a set of springs. The stiffness of these springs can be determined from the elastic properties of the plate material. Compression of the paper structure proceeds by lowering the rigid top surface of the pressing plate in small steps of size Δz_p . At the end of each step, the surface profiles of the pressing plate and paper structure are adjusted so that every spring in the system remains in mechanical equilibrium. The fibres in the bulk

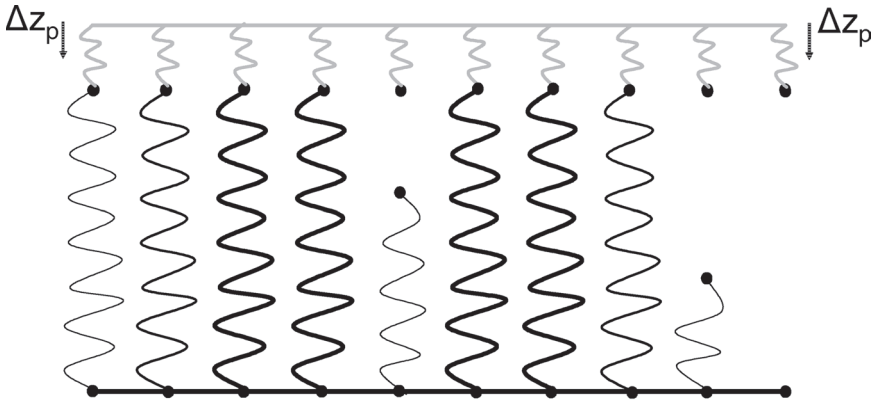


Figure 2 Discretization of the paper-plate system of Figure 1 using the spring-field model of Provatat and Uesaka.

undergo homogeneous deformations which are calculated from the local strain value. The process continues until the caliper of the paper or the pressure applied by the plate has reached a certain value.

There are several limitations to this approach. The first problem, which can be easily fixed, is that the contact problem was only solved on one surface rather than on both the top and bottom surfaces. A second, more serious issue is that neighbouring springs move independently of each other. That assumption only holds if the distance between the springs is greater than the length over which paper deformations are correlated in the XY plane. Finally, and perhaps most importantly, the approach neglects fibre-level deformations inside the sheet structure. This is crucial when the phenomena in question are in the length scale of fibre width (or even less), such as a half-tone definition, fibre wicking, missing dots, and surface roughening, as seen in many issues related to printing. In the next section, we introduce a new consolidation model that resolves all of these issues and preserves the entire three-dimensional fibre-network during compression.

STOCHASTIC MODELLING OF PAPER STRUCTURE AND COMPRESSION

In this new algorithm, Hookean springs are used to model the compressibility of individual fibres rather than whole sections of the fibre network. The model also accounts for shear forces in the thickness direction. This is

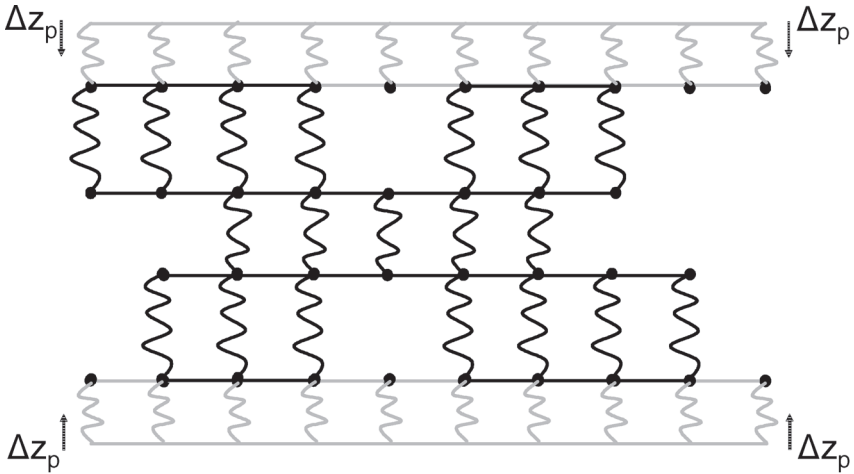


Figure 3 Discretization of the paper-plate system of Figure 1 using the proposed algorithm.

accomplished by connecting neighbouring nodes on the surfaces of the fibres and plates with shear elements, shown as solid line segments in Figure 3. As seen from the figure, both the top and bottom pressing plates are now discretized, and their elastic properties can be set to reflect the type of consolidation process that is studied. For example, to simulate the compression of a sheet in a gravure printing nip, one would combine a hard, top plate (gravure cylinder) and a soft, bottom plate (impression roller). The plates can also have non-planar surfaces, e.g., when simulating the effect of wet pressing, the profile of a pressing felt can be used to model the surface of one of the pressing plates.

The spring and shear stiffness of the fibres can be determined from measurements performed on individual pulp fibres. In the model, these quantities are allowed to vary from fibre to fibre, e.g., fibres with a thick cell wall can be made less compressible than those with a thinner wall.

As in the previous model [4], an iterative procedure is used to consolidate the fibre network. At the start of each step, the nodes on the outer surfaces of the pressing plates are moved by an amount Δz_p towards the center of the paper. To determine how the paper structure and plate surfaces deform following that displacement, one must consider the forces acting on each node in the system. Consider for example the small section of fibre shown in Figure 4. Node 1 in the drawing is connected by shear elements to four other nodes on

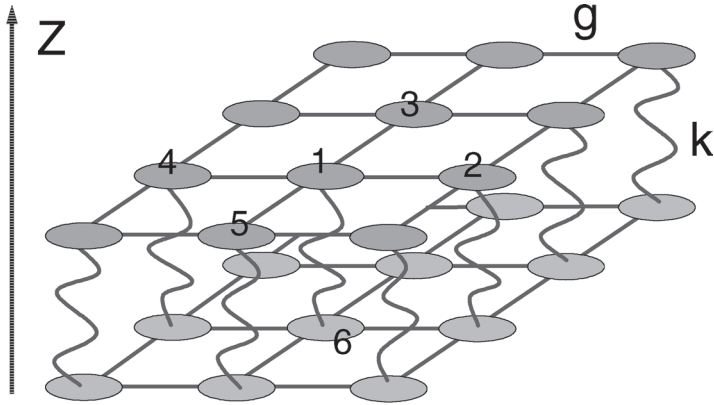


Figure 4 Schematic representation of a fibre, showing how nodes on its top and bottom surfaces are connected in the new model.

the top surface of the fibre and it is also connected by a spring to node 6 on the bottom surface of the same fibre.

Assuming that each element contributes a force that is linear in the relative displacement of the two nodes it connects, the total force acting on node 1 can be written as

$$F_1 = k(\Delta z_6 - \Delta z_1) + g(\Delta z_2 - \Delta z_1) + g(\Delta z_3 - \Delta z_1) + g(\Delta z_4 - \Delta z_1) + g(\Delta z_5 - \Delta z_1), \quad (1)$$

where g and k denote the shear and spring stiffness of the force elements, respectively. Similar expressions can be obtained for every node in the system. In this work, we assume that the paper and plates remain in quasi-static equilibrium throughout the consolidation process, i.e., we set $F_i = 0$, where i denotes any node in the paper or on the inner surfaces of the plates. The resulting equations for the unknown displacements Δz_i form a sparse linear system which can be written in matrix form as $\mathbf{A} \cdot \Delta \mathbf{z} = \mathbf{b}$, where $b_i = k_{tp} \Delta z_p$ if node i is on the inner surface of the top pressing plate, $b_i = -k_{bp} \Delta z_p$ if it is on the inner surface of the bottom plate, and $b_i = 0$, otherwise. We find the solution to this linear system using a bi-conjugate gradient method [14]. The accuracy of the numerical solution is set by a convergence parameter ϵ such that the displacements $\Delta \mathbf{z}$ satisfy the inequality $|\mathbf{A} \cdot \Delta \mathbf{z} - \mathbf{b}| / |\mathbf{b}| < \epsilon$. Once the displacements have been found, the position of every node in the system is updated, and new points of contact between the pressing plates and the network or between fibres in the bulk are identified. The stiffness of the spring and shear elements in each fibre can also be adjusted to yield a particu-

lar stress-strain curve or to reflect a change in fibre morphology. For example, the springs can be made very stiff in locations where the lumen is collapsed. Once the configuration of the system has been updated, another consolidation step is taken and the process continues until the caliper of the paper or the pressure applied by the plates has reached some predetermined value.

In some cases, for example when a paper web goes through a nip at very high speeds, the condition of quasi-static equilibrium may not be satisfied. In such cases, one may gain some insight into the dynamics of the paper-plate system by solving instead the set of equations

$$\frac{1}{\tau} \frac{dz_i}{dt} = F_i, \quad \frac{dz_{tp}}{dt} = -v_{tp}, \quad \frac{dz_{bp}}{dt} = v_{bp}, \quad (2)$$

where z_{tp} and z_{bp} locate the outer surfaces of the top and bottom pressing plates, and v_{tp} and v_{bp} denote the speed at which these rigid surfaces are moving. The quantity τ is a relaxation rate that characterizes how quickly the nodes relax to their equilibrium configuration. When that rate is large, the system remains close to equilibrium at all times and the consolidation process becomes quasi-static. In that limit, the equations given above become equivalent to the Jacobi relaxation method for solving the equations $F_i = 0$. The Jacobi method being slower than the bi-conjugate gradient technique mentioned above [15], we have used the latter throughout this work and have not yet considered cases in which the system is out of quasi-static equilibrium.

Once the target load or caliper has been reached, the compression process is stopped and the pressing plates are retracted from the paper. As before, the process is decomposed into a series of small steps during which the system is assumed to remain in mechanical equilibrium. It is possible to control the amount of strain recovery that occurs during unloading by adjusting the stiffness of the springs and shear elements inside the paper before the process starts. For example, most of the deformation occurring during compression can be made permanent through a large increase in stiffness. At the end of each step, the distribution of load on the two surfaces of the paper is updated, and the paper and plates are separated from each other where the load has become negative. At present, we assume that all fibre-fibre contacts in the bulk are preserved during unloading. The process continues until the paper and plates are completely detached from each other.

The most basic assumption made in this proposed model is that each node is displaced only in the Z-direction. The location of each node in the XY plane is determined during fibre deposition and restricted to points on a two-dimensional rectangular grid (the distance between neighbouring points on that grid must be smaller than the width of the deposited fibres). In other

words, space is discretized in the X and Y directions but it is treated as a continuum in the Z-direction. Since the nodes are not allowed to move in-plane, there are no Poisson effects and no bending or twisting moments of the fibres. This assumption may be valid in a bulk scale for highly layered structures, such as paper. For example, Mann et al. [16] showed that the Poisson ratio of a paperboard for the Z-direction compression is extremely small compared to the corresponding in-plane components. However, it may not be generally true at a micro-scale. An estimate of the magnitude of the errors from this assumption requires full structure modelling.

MICRO-SCALE CONTACT MECHANICS

As a first application, we have used the model presented above to study the uniformity of contact between the surface of a paper and that of a pressing plate. The main objective of this work is to determine which paper properties can best predict non-contact areas between the paper and plate at different pressing pressures. In printing applications, these non-contact areas determine the overall print density, dot definition (image sharpness), and missing dots in gravure prints.

The first step in the study was to generate three-dimensional paper structures with realistic bulk and surface properties. We accomplished this by first depositing 860 fibres over a square area of size 1 mm^2 , decomposed into 200×200 grid points spaced $5 \text{ }\mu\text{m}$ apart. The dimensions of the fibres were chosen to represent a hardwood species such as aspen: average length $700 \text{ }\mu\text{m}$, width $20 \text{ }\mu\text{m}$, thickness $8 \text{ }\mu\text{m}$ and cell wall thickness $2.5 \text{ }\mu\text{m}$. For a coarseness of 0.1 mg/m , the simulated structure corresponds to a sheet with a basis weight of about 60 g/m^2 . The deposited network was then compressed to a predetermined caliper using the new consolidation algorithm. In this particular study, we used a single spring stiffness k_f for all fibres and tentatively set $k_f = g_f$, even though ideally these constants should be estimated from separate measurements performed on individual fibres. In a series of experiments performed on single wet fibres under transverse compression, Wild et al. [17] showed that the spring stiffness of the fibres during cell wall compression was up to twenty times larger than during the initial stages of compression. Eventually, we plan to use data from force versus thickness curves such as those given in Ref. [17] to progressively increase the spring stiffness of the fibres during compression. In the simulations presented below, we have simply increased the local spring constant by a factor of ten once the lumen was collapsed. In the model, the relative stiffness between the pressing plates and fibres determines how much each one will deform when they are pressed

together. A realistic description of the plate system used in wet pressing would combine a hard, flat plate and a soft, textured material such as a press felt or blotter. Since the objective here was not to simulate the process of wet pressing but rather to consolidate the deposited fibre network to a realistic density, we have assumed instead that the two flat plates were identical and relatively soft, and set $k_p/k_f = 5$ and $k_p = g_p$, where k_p and g_p denote the compression and shear stiffness of the two pressing plates. Discretization of the fibre network and of the two pressing plates required roughly 1.1 million nodes. The two pressing plates were moved in steps of size $\Delta z_p = 0.2 \mu\text{m}$ until the caliper of the network had decreased from an initial value of $241 \mu\text{m}$ to $75 \mu\text{m}$. Prior to unloading, the stiffness of all the shear elements inside the paper was increased by a factor of ten. Springs whose stiffness had not changed during consolidation were also made ten times stiffer. Following strain recovery, the paper had bounced back to a caliper of $88 \mu\text{m}$ and the rest remained as a plastic compressive strain that represents “consolidation”. The top and bottom surfaces of that final paper structure have realistic rms (root mean square) roughness values of 4.42 and $3.46 \mu\text{m}$, respectively.

Part of the cross-section of that structure is shown in Figure 5, while the top surface of the paper and the formation (mass density distribution) of the sheet are shown in Figures 6A and 6B. In these two figures, the red colour denotes highest surface or highest mass density areas. Mass density is measured as the number of fibres deposited over a given point in the XY plane.

The calculation took roughly 6 hours on a computer with a processor

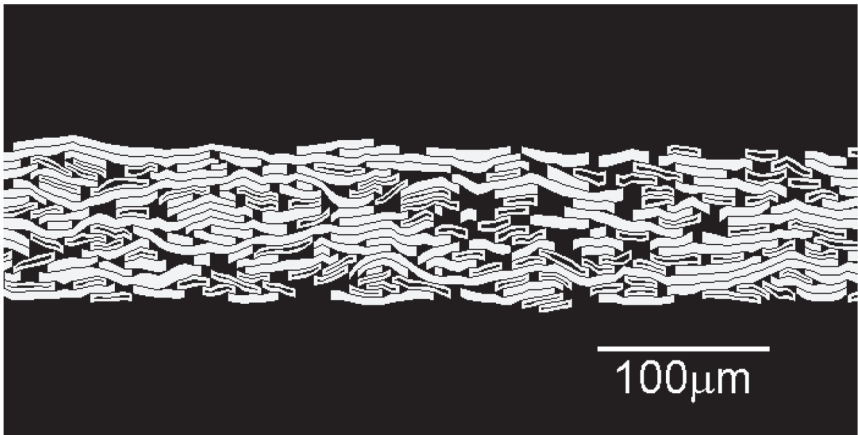


Figure 5 Part of the cross-section of a simulated paper structure.

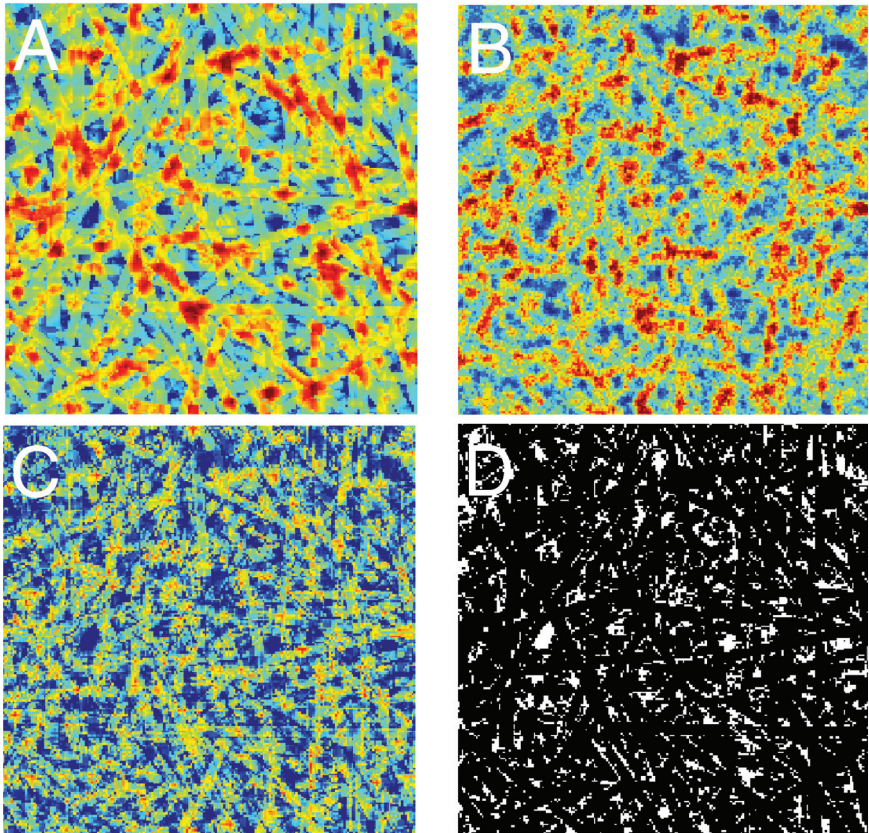


Figure 6 A) Surface profile of the top side of a simulated paper sheet covering an area of size 1 mm^2 . B) Spatial variation of local mass density for the same structure. C) Nodal force (pressure) distribution on the top surface of the paper at a strain of 33% D) State of contact between paper and plate at the same strain value. Non-contact areas are shown in white.

speed of 3.06 GHz when the convergence tolerance ε was set to 10^{-4} . The same calculation took only 2 hours when ε was set to 10^{-3} while the surface profiles of the structures obtained in the two cases differed by less than 0.2%.

The paper structure generated in the simulation described above was then compressed a second time between two pressing plates to simulate printing. The results presented below correspond to a case in which the top pressing

plate is hard ($k_{ip} = g_{ip} = 50k_f$), while the bottom plate is relatively soft ($k_{bp} = g_{bp} = 5k_f$), as happens in a gravure printing nip. However, results obtained when compressing the structure between two hard ($k_{ip} = g_{ip} = k_{bp} = g_{bp} = 50k_f$) or two soft plates ($k_{ip} = g_{ip} = k_{bp} = g_{bp} = 5k_f$) were qualitatively similar. Throughout these simulations, we monitored the pressure distribution on the paper surfaces as well as the area of contact between the paper and the two plates. Figures 6C and 6D show both fields measured on the top side of the paper at a compressive strain of about 33%.

We looked for correlations between the local value of these two fields and that of various structural properties of the uncompressed sheet, such as local mass density, caliper and surface height. The coefficient of correlation between the pressure distribution and each one of these sheet properties is shown on Figure 7A as a function of the total displacement of the top pressing plate. We found positive correlations between the pressure distribution and the top surface profile (open circles), as well as between the pressure and either local mass density (open squares) or local thickness (open triangles). In all three cases, the coefficient of correlation increases with contact area from a very small value to a maximum which is just above 0.7 in the case of the top surface profile.

It is possible to obtain a coefficient of correlation that is more or less

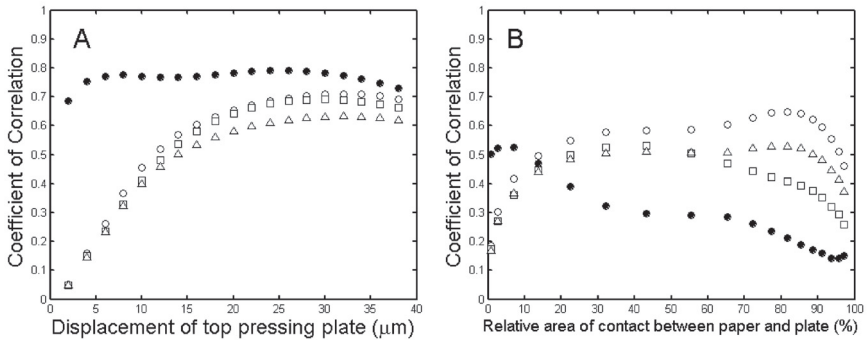


Figure 7 A) Coefficient of correlation between pressure distribution and three different sheet properties: surface height (open circles), local mass density (squares) and thickness (triangles). The filled circles represent the coefficient of correlation between the pressure distribution and the function $F(x,y)$ defined in Equation (3). B) Coefficient of correlation between the contact state $C(x,y)$ and surface height (open circles), local mass density (squares) and thickness (triangles). Correlations between $C(x,y)$ and the function $C_h(x,y)$ defined in Equation (4) are shown with filled circles.

constant over the entire compression range by assuming that the load at point (x,y) is proportional to the product of the local mass density and the total compression of the surface at that point. Explicitly, we assume that the load at point (x,y) is proportional to the function

$$F(x,y) = \begin{cases} \rho(x,y)[h(x,y) - h_{tp}] & \text{if } h(x,y) > h_{tp}, \\ 0 & \text{otherwise.} \end{cases} \quad (3)$$

In Equation (3), $\rho(x,y)$ is the mass density at point (x,y) , $h(x,y)$ is the local height of the surface before compression and h_{tp} is the position of the top pressing plate, which changes in time. In writing down the above expression, we have naively assumed that a point on the paper surface is in contact with the pressing plate if its height before compression is above the current location of the plate, which is treated as incompressible. This is equivalent to assuming that the non-contact areas do not deform in response to the stresses applied on the areas of contact. As we will show below, this is a rather drastic approximation. In spite of this, the coefficient of correlation between the measured pressure distribution and $F(x,y)$ remains close to 0.75 over most of the compression range (solid dots in Figure 7A).

The micro-scale pressure distribution, such as measured in this example, may affect gloss development during calendering. The results obtained here demonstrate that the local pressure is strongly influenced by the local mass density as well as the local surface height. Thus, formation, defined here as mass density distribution, is an important parameter to control the micro-scale pressure variations, as is often claimed in macroscopic formation measurements [18] (It should be noted that formation on this length scale, say $5 \mu\text{m}$, is not measured by most commercial equipment).

In conventional printing processes and in particular in gravure printing, non-uniformities in ink transfer may be more closely related to the state of contact between the paper and printing plate than to the pressure distribution on the paper surface. In the calculations presented below, that state of contact is represented by the field $C(x,y)$ which is set to 1 at points of contact between the paper and plate and 0 elsewhere. Figure 7B shows how the coefficient of correlation between $C(x,y)$ and the properties of the uncompressed sheet varies with the area of contact between the paper and plate. As before, correlations with surface height are represented by open circles, while open squares and triangles are used for mass density and caliper, respectively. In the case of surface height and caliper, the coefficient of correlation initially increases with the relative contact area f_A , then stays more or less constant over a wide range of values of f_A before decreasing again rather sharply as the

contact area becomes larger than 85%. In the case of formation, the decrease in the coefficient of correlation starts at around $f_A=50\%$. In all cases, the coefficient never increases above 0.7, suggesting that none of these conventional sheet properties can predict very accurately the contact and non-contact states. The fourth curve on the graph shows the coefficient of correlation between $C(x,y)$ and the function

$$C_h(x,y)=\Theta [h(x,y)-h_p]. \quad (4)$$

The Heaviside step function $\Theta(u)$ in Equation (4) is equal to one if u is positive and 0 if u is negative. The basic assumption here is that the paper and plate come into contact locally when the plate height becomes less than the *initial* surface height of the sheet. As shown in the figure, the coefficient of correlation between C and C_h , which is around 0.5 at a contact area below 1%, steadily decreases as the area of contact between the paper and plate increases. This decrease is due to the fact that the non-contact areas deform in response to the pressure applied by the top pressing plate. As a result, one cannot accurately predict the state of contact of a point on the surface by just considering its height before compression. In addition, we found that contact on the top side of the paper can be affected by what happens on the bottom side. This is especially true in the early stages of compression, when the two pressing plates are only in contact with a few points on the top and bottom surfaces of the paper. In these early moments, the pressure applied by a plate at a point of contact with the paper surface causes the paper structure in the area of contact to ‘translate’ towards the other plate. Local surface and bulk deformations become important only when both sides of the paper achieve contact with the pressing plates. Since this effect is absent from Equation (4), it is not surprising that the coefficient of correlation we measure is small even in the early stages of compression.

These results suggest that the state of contact between a paper surface and a pressing plate cannot be predicted by simply considering the topography of the surface. Since the simulation model developed here provides the full structural and mechanical information at the microscopic scale (most of which is not accessible to existing experimental techniques), it provides a promising approach to find new predictive parameters involving both surface and bulk properties.

CONCLUDING REMARKS

We have proposed a new model for predicting how a stochastic paper structure deforms under compression. Since this model preserves the entire three-dimensional structure of the sheet during compression, it provides a description of fibre-level deformations both on the surfaces of the network and inside the bulk. The model can easily accommodate soft and hard pressing plates of varying stiffnesses, and *textured* plates (e.g., pressing felts). These features will be particularly useful when simulating wet pressing, and for predicting, for example, felt marks or two-sidedness in surface properties. In the area of calendering, possible applications include predicting how different roll covers will affect smoothness development and local density variations. As a first application, we considered the contact mechanics between a pressing plate and a paper surface and found that the surface profile and mass density distribution were important parameters in predicting the pressure distribution on the paper. The study also showed that the pressure applied by the pressing plates affects not only the contact area but also the non-contact area of the paper surface. Finally, it was found that the contact state on one side of the paper can be influenced by that on the other side. In many applications, the compression algorithm developed here will require data for several properties of both dry and wet fibres. Experimental determination of these properties and a series of simulations are currently underway.

ACKNOWLEDGMENTS

The authors would like to thank Paul Shallhorn for his comments on the manuscript.

REFERENCES

1. I. Endres. Compression uniformity measurements on coated and uncoated paper surfaces, Licentiate thesis, Department of Chemical Engineering, Karlstad University, Karlstad, 2004.
2. P.J. Mangin, M.C. Beland, and L.M. Cormier. A structural approach to paper surface compressibility – Relationship with printing characteristics. In **Products of Papermaking**, *Trans. 10th Fund. Res. Symp.*, (ed. C.F. Baker), Vol. 3, pp 1397–1427, Pira International, Leatherhead, UK, 1993.
3. K. Niskanen and M.J. Alava. Planar random networks with Flexible Fibers. *Phys. Rev. Lett.* **73**(25):3475–3478, 1994.

4. N. Provatas and T. Uesaka. Modelling paper structure and paper-press interactions. *J. Pulp and Paper Sci.* **29**(10):332–340, 2003.
5. O. Kallmes and H. Corte. The structure of paper. *Tappi J.* **43**(9):737–752, 1960.
6. H. Corte and O.J. Kallmes. Statistical geometry of a fibrous network. In **The Formation and Structure of Paper**, *Trans. 2nd Fund. Res. Symp.*, (ed. F. Bolam), Vol. 1, pp13–52, BPBMA, London, 1962.
7. J. Görres, C. S. Sinclair and A. Tallentire. An interactive multi-planar model of paper structure. *Paperi ja Puu* **71**(1):54–59, 1989.
8. M. Deng and C. T. J. Dodson. Chap. 3 in **Paper: An engineered stochastic structure**, Tappi Press, Atlanta, 1994.
9. W.W. Sampson. The statistical geometry of fractional contact area in random fibre networks. *J. Pulp and Paper Sci.* **29**(12):412–416, 2003.
10. L.H. Switzer, D.J. Klingenberg and C.T. Scott. Handsheet formation and mechanical testing via fibre-level simulations. *Nordic Pulp Paper Res. J.* **19**(4):434–438, 2004.
11. K. Niskanen, N. Nilsen, E. Hellen and M. Alava. KCL-PAKKA: Simulation of the 3D structure of paper. In **The Fundamentals of Papermaking Materials**, *Trans. 11th Fund. Res. Symp.*, (ed. C.F. Baker), Vol. 2, pp1273–1291, Pira, Surrey, 1997.
12. N. Provatas, M. Haataja, J. Asikainen, S. Majaniemi, M. Alava, and T. Ala-Nissila. Fiber deposition models in two and three spatial dimensions. *Colloids Surf. A* **165**:209–229, 2000.
13. U. Aaltosalmi, M. Kataja, A. Koponen, J. Timonen, A. Goel, G. Lee, and S. Ramaswamy. Numerical analysis of fluid flow through fibrous porous materials. *J. Pulp and Paper Sci.*, **30**(9):251–255, 2004.
14. W. H. Press, S. A. Teukolsky, W. T. Vetterling, and B. P. Flannery. Chap. 2 in **Numerical Recipes in Fortran 77**, Cambridge University Press, 1992.
15. G. G. Batrouni and A. Hansen. Fourier acceleration of iterative processes in disordered systems. *J. Stat. Phys.* **52**:747–773, 1988.
16. R.W. Mann, G.A. Baum, and C.C. Habeger. Determination of all nine orthotropic elastic constants for machine-made paper. *Tappi*, **63**(2), pp163–166 (1980).
17. P. Wild, I. Omholt, D. Steinke and A. Schuetze. Experimental characterization of the behaviour of wet single wood-pulp fibres under transverse compression. *Paprican University Report*, PUR 862, 2004.
18. T. Koskinen, Calender blackening. 2nd EcoPaperTech, International conference on economy and ecology in papermaking technology, pp207–218, Helsinki, Finland, June 1998.

Transcription of Discussion

A STOCHASTIC STRUCTURE MODEL FOR PREDICTING SHEET CONSOLIDATION AND PRINT UNIFORMITY

François Drolet¹ and Tetsu Uesaka²

¹Pulp and Paper Research Institute of Canada, Pointe-Claire, Qc, Canada

²Mid Sweden University, FSCN, Sundsvall, Sweden

Jean-Claude Roux EFPG-INPG

Very nice work and very interesting. I was wondering how you determine or identify your coefficients k and g in the model? Another question which is related to the previous one. You seem to have exactly the same coefficient in machine direction and cross direction. Can you comment on this?

François Drolet

For the spring stiffness k , we have used experimental data obtained by Peter Wild and his group at the University of Victoria. His experimental setup consists of an anvil and a hammer which he uses to compress individual fibres and obtain force versus compression curves. Peter was kind enough to make most of his data available to me, so I can actually take his curves and feed them directly into the model. For the shear stiffness there is very, very little data available. Peter, Ingunn Omholt and I have been discussing recently how we could possibly modify his experimental setup to measure shear stiffness instead. At present, however, I usually assume that $g = k$.

As for the difference between machine and cross machine directions, it is accounted for during fibre deposition. For example, the orientation of each fibre can be chosen from a non-uniform distribution with a maximum along the machine direction. During compression however, we do not adjust the

Discussion

stiffness of the fibres according to their orientation. At present, we also use the same shear stiffness along the length of the fibre and along its width.

Tomas Larsson STFI-Packforsk AB

I have a rather simple question about the first model you showed, the one with just five fibres. When you compressed that one, you can see that two fibres came together. If you unload that structure will they separate?

François Drolet

Very good question. The answer is that at present, no. It is an important point since it affects the amount of strain recovery that actually takes place. Right now, when I unload, all the contacts inside the structure are preserved. In the real system, many fibre-fibre contacts probably disappear during unloading and so we will have to modify the model to include that possibility. I should point out that the model does allow nodes on the pressing plates to separate from nodes on the surface of the paper during unloading. We just need to implement a similar procedure in the bulk.

Marit Van Lieshout Paperlinx

Stephen I'Anson and I have had this discussion about rewetting. That is, whether the water remains within the sheet or whether it goes out of the sheet and flows back in again. The main question is whether there is enough room in these non-compressed areas for all this water? What does your model say about this?

François Drolet

The model does not say anything about fluid flow at present. But we would definitely like to study how, for example, dewatering affects the network structure during wet pressing.

Marit Van Lieshout

You showed an image of the places where you did not compress. They were big, and higher bulk. Do you know anything about the volumes in this higher bulk areas?

François Drolet

No, I did not look at those areas, but that would be interesting. I should mention that we are currently developing tools to better characterize the three-dimensional structures obtained with our model. For example, we are implementing algorithms to measure the three-dimensional pore size distribution and the permeability of the sheet. Such tools are essential since they provide a quantitative description of the fibre network that goes beyond the nice pictures.

William Sampson University of Manchester

Quite often when you have repeated compression and relaxation of a web, then you will see less recovery of the web with repeated compressions and at the moment your model would not allow this unless you change the stiffness of the fibres, am I correct?

François Drolet

That is correct, yes, you have to change the stiffness of the fibres. I should mention that Peter Wild has done several experiments involving cyclic compression of single pulp fibres so again, I could use some of his data as input for my simulations.

William Sampson

It would be nice not to be so dependant on experimental data for each thing you sought to understand.

Patrice Mangin

I would like to thank you for this wonderful modeling as it will help us to learn a lot more about paper as a product, notions that are very difficult to understand from experiments. Hopefully and eventually, you could use some of the data from the cyclotron and use these as a base sheet which would be real in this case.

François Drolet

Yes, that would be very interesting to do.